Project acronym:	**Geo-Drill**		
Project title:	Development of novel and Cost-Effective drilling technology for geothermal Systems		
Activity:	LCE-07-17-Renewables		
Call:	H2020-LC-SC3-2018-RES-TwoStages		
Funding Scheme:	RIA	**Grant Agreement No:**	815319
WP7	Simulation, KBS and DSS		

D7.1 Geothermal Well Flow Assurance Simulator

Due date:	30/11/2020 (M20)	
Actual Submission Date:	29.01.2021	
Lead Beneficiary:	FPS	
Main authors/contributors:	FPS	
Dissemination Level[1]:	PU	
Nature:	Report	
Status of this version:		**Draft under Development**
		For Review by Coordinator
	X	**Submitted**
Version:	01	

REVISION HISTORY

Version	Date	Main Authors/Contributors	Description of changes

Funded by the Horizon 2020 Framework Programme of the European Union

1

Dissemination level security:

PU – Public (e.g. on website, for publication etc.) / **PP** – Restricted to other programme participants (incl. Commission services) / **RE** – Restricted to a group specified by the consortium (incl. Commission services) / **CO** – confidential, only for members of the consortium (incl. Commission services)

This project has received funding from the European Union's Horizon 2020 program Grant Agreement No 815319. This publication reflects the views only of the author(s), and the Commission cannot be held responsible for any use which may be made of the information contained therein.

Document: D7.1 Geothermal Well Flow Assurance Simulator

Version: 1

Date: 29.01.2021

Summary

A new engineering analysis software for geothermal flow assurance is under development by Flowphys AS. This software is capable of simulating single-phase and multi-phase dynamic (time-dependent) flows in complex pipe networks and is based on conservation equations. Part of the software development is carried out in several H2020 projects: GeoCoat, GeoSmart, GeoPro. In the Geo-Drill project, this software is further extended and improved, with a focus on features needed to simulate drilling operations and to function in conjunction with the drill physics simulator and drill monitor in Tasks T7.2-T7.4.

In this report, the fundamentals of the flow assurance software, Flowphys1D, are first briefly summarised. This is followed with more detailed descriptions of the new models that have been developed for non-Newtonian fluids, flow and heat transfer in the annulus, and for the hammer tool assembly. In addition, the report also describes a Drill Module GUI which has been developed to simplify and speed-up end-user input for construction of the well and drill string geometries and meshes.

Objectives met

The work described in this report contributes to the following WP7 objective:

- To develop geothermal well flow assurance simulator.

CONTENTS

1. INTRODUCTION

Flow assurance simulation originates from the oil and gas industry, where it is used to analyse multi-phase flows in oil and gas pipe networks. It is in many ways similar to process engineering simulations, with pipe network issues such as determination of pipe diameters, pressure drops, devices such as pumps, separators, valves, heat exchangers, etc. However, it differs in that it has a stronger focus on multi-phase flows, also including transients, as well as the ability to analyse and predict solid deposits (hydrates, scaling, wax), structural integrity (corrosion, erosion), flow regimes (e.g. slugging), and operational procedures such as injection of inhibitors, etc. The requirements of flow assurance necessitate reasonably fine discretisation along the pipes.

A dynamic (time-dependent) two-phase pipe network flow assurance simulator for geothermal powerplants is under development by Flowphys AS. This development is partly financed by H2020 projects GeoCoat, GeoSmart, and GeoPro. In the GeoDrill project, this simulator has been extended with new models for non-Newtonian fluids, flow in annulus, simplified model for the hammer tool assembly, and a GUI module for drilling operation simulations. In this report, a summary of the flow assurance simulator's underlying methods is presented, followed with more details for the extensions developed in the GeoDrill project.

2. GEOTHERMAL FLOW ASSURANCE SIMULATOR

2.1 Governing Equations and Solution Methods

This section introduces the governing equations and solution methods and is a brief summary of the Geo-Coat project report [1]. The conservation equations for mass, momentum, and energy form the governing equations to be solved. For single-phase flows, they can be written as

$$A\frac{\partial \rho}{\partial t} + \frac{\partial \dot{m}}{\partial x} = 0\,, \tag{2.1}$$

$$\frac{\partial \dot{m}}{\partial t} + \frac{\partial v\dot{m}}{\partial x} + A\frac{\partial p}{\partial x} + \rho g A\frac{\partial z}{\partial x} + \frac{f\dot{m}|\dot{m}|}{2\rho DA} = 0 \tag{2.2}$$

$$\frac{\partial}{\partial t}(\rho CTA) + \frac{\partial}{\partial x}(CT\dot{m}) = \frac{\partial}{\partial x}\left(kA\frac{\partial T}{\partial x}\right) + \phi \tag{2.3}$$

where $\dot{m}$ is the mass flow rate, ρ is the fluid density, v is the velocity, A is the cross-section area of the pipe, D is the pipe diameter, f is the Darcy-Weisbach friction factor, T is the absolute fluid temperature, C is the specific heat capacity, k is the thermal conductivity and ϕ is the heat flux through the pipe wall.

For pipe networks, extra conditions are needed at junction nodes. These can be chosen in different ways. In the FlowPhys1D code, we have chosen to conserve mass flow rate $\dot{m}$ and heat flux q. Thus, for a junction with k pipes, the following equations are fulfilled:

$$\sum \dot{m}_k = 0 \tag{2.4}$$

$$\sum q_k = 0 \tag{2.5}$$

In addition, the pressure p and temperature T are also required to have the same values at the junction node. These requirements are illustrated in Figure 2.1 for the case of a junction node with three pipes.

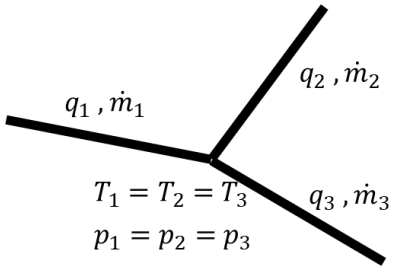

Figure 2.1: Conditions fulfilled at junction nodes

The pipe network flow solver uses several different steps and iterations to carry out the simulations. First a steady state solution is calculated using simplified equations and chemistry to get a good initial condition. This is followed by time-stepping, where each timestep uses Newton-Raphson (N-R) iterations for the non-linear equations. In each timestep, the mass flow and pressure equations (i.e. mass conservation and momentum conservation equations) are solved in a strongly coupled fashion (i.e. both appear together in the system matrix). Similarly, the heat flow and temperature equations (i.e. energy conservation equation) are also solved in a strongly coupled fashion. The combined mass flow, pressure, heat flow, and temperature equations are then solved sequentially and loosely coupled via Newton-Raphson equilibrium iterations. The fluid properties are calculated at the start of each timestep and kept constant during the N-R iterations.

2.2 **Geofluid models**

Several different options have been implemented into the FlowPhys Flow Assurance Simulator to calculate fluid properties and the dependence on temperature, pressure, and chemical composition:

- Constant properties
- Relations for properties of pure water
- PVT (Pressure-Volume-Temperature) tables
- PHREEQC for aqueous geochemical calculations

Of these, the most powerful option is PHREEQC, an open-source software for aqueous geochemical calculations developed by USGS [2]. One part of the software is PhreeqcRM, a subroutine library for coupling PHREEQC to reactive-transport simulators, which allows access to all PHREEQC reaction capabilities. It contains methods for initial and boundary conditions, running reactions, transfer of data to and from the module, and parallelisation by MPI or OpenMP. The PhreeqcRM subroutines can be called directly from a Fortran program, and require no additional coupling software.

2.3 **Device models**

The simulator uses a range of models for calculating mass flow, pressure, temperature in pipes and devices. Some of these models are:

- Pump
- Valve
- Turbine

- Fan
- Heat Exchanger
- Separator
- Well

2.4 Flow Assurance GUI

An extensive GUI is currently under development for the flow assurance solver in several different H2020 projects (GeoCoat, GeoDrill, GeoSmart, GeoPro). The GUI includes creation of conceptual piping diagrams, modelling of actual 3D geometries and pipe layouts, meshing, simulation management, post-processing of results, optimisation, etc. An example of a screenshot of a simple schematic geothermal powerplant mesh is shown in Figure 2.2.

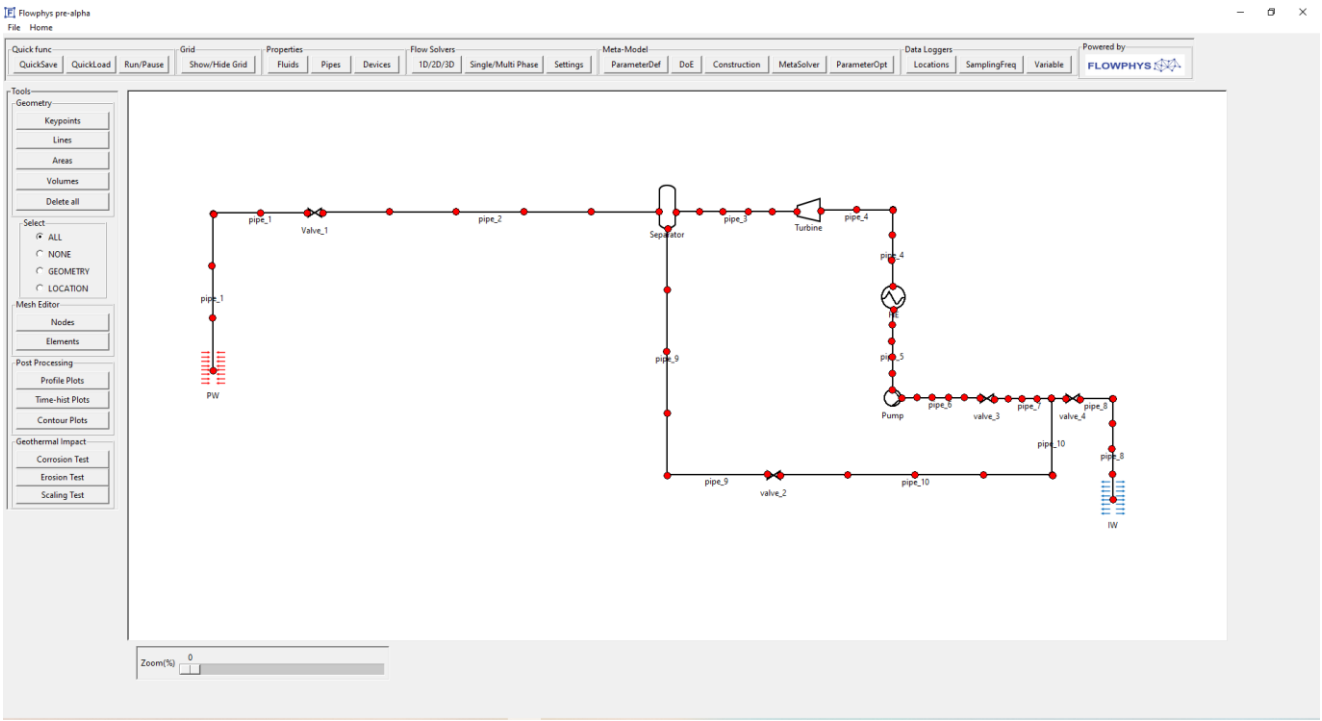

Figure 2.2: Example of a flow assurance model and mesh in the Flowphys1D GUI

3. GEOTHERMAL FLOW ASSURANCE SIMULATOR: GEO-DRILL ADDITIONS

3.1 Drill Module GUI

To simplify the creation of wells and drill strings, a drill module GUI has been developed. Sample screen shots are shown in Figure 3.1 and Figure 3.2. These are from a pre-alpha version; the drill module is still in development and will undergo further changes and additions before being released.

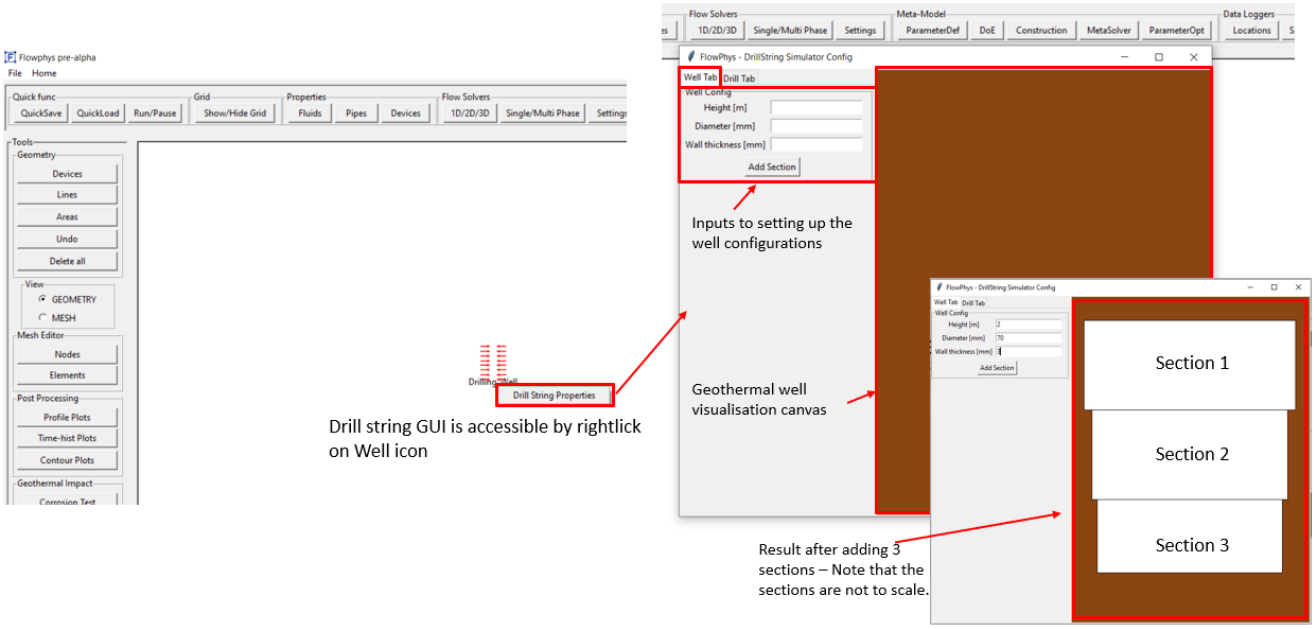

Figure 3.1: Flowphys1D drill string analysis module GUI: creating well

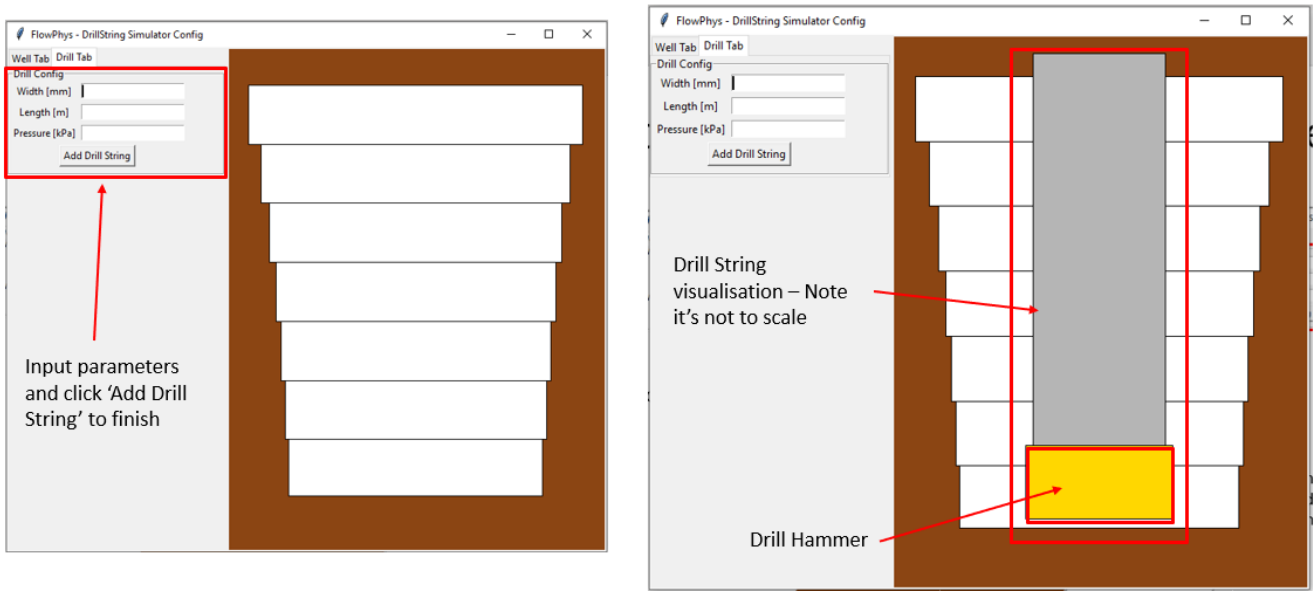

Figure 3.2: Flowphys1D drill string analysis GUI: creating well with drill string

3.2 Non-Newtonian fluids

3D implementation:

For a Newtonian fluid, the shear stress is directly proportional to the shear rate,

$$\tau_{ij} = \mu\gamma_{ij} \tag{3.1}$$

where μ is the absolute or dynamic viscosity, which may be constant or depend on temperature and pressure, and γ is the shear rate. While this is mostly an adequate description of gases and many common liquids such as water, it may, in some cases, not be accurate enough for drilling fluids, which typically behaves as non-Newtonian fluids. To simulate such fluids, non-Newtonian fluid models were developed and implemented into the Flowphys3D software, see GeoDrill report D4.1 [3]. The main model implemented is the Herschel-Bulkley model, which can be seen as a combination of a power law model and a Bingham plastic model, see Figure 3.3.

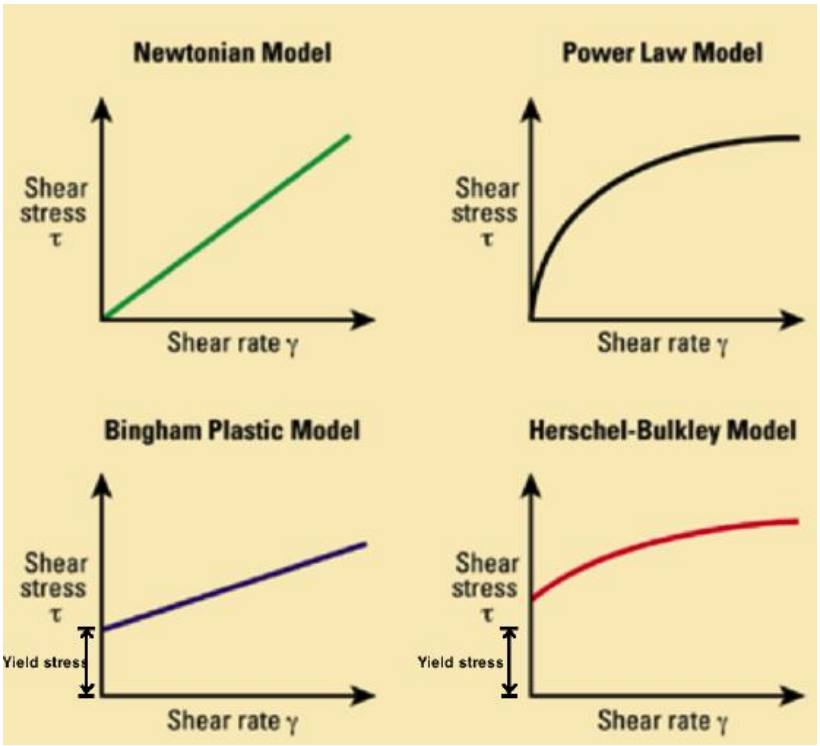

Figure 3.3: Behaviour of different fluid models [4]

The shear rate dependent viscosity of the Herschel-Bulkley model is calculated as

$$\mu(|\dot{\gamma}|) = \begin{cases} \infty & \text{for} \quad |\tau| < \tau_0 \\ K|\dot{\gamma}|^{n-1} + \dfrac{\tau_0}{|\dot{\gamma}|} & \text{for} \quad |\tau| \geqslant \tau_0 \end{cases} \tag{2}$$

where τ_0 is the critical shear stress below which the fluid behaves as an elastic solid, meaning that it does not flow, K is referred to as the consistency index, and n the behaviour index. Notice that for $n = 1$, $K = \mu$, and $\tau_0 = 0$, the constant viscosity of a Newtonian fluid is obtained.

For the drilling fluid tested in the GeoDrill D1.3 Rheology testing report [5], the Herschel-Bulkley model parameters were calculated via a least squares curve fitting to the experimental data, see GeoDrill

D4.1 [3]. However, the curve fitting in D4.1 was mainly aimed at high shear rates, which resulted in shear thickening. For drilling operations, the shear rate would typically be lower, and the drilling fluid have a shear thinning behaviour. For example, for water flowing in a pipe with diameter 150 mm with flow rate 600 L/min, the shear stress is < 0.9 Pa.

Using the least squares fit of the Herschel-Bulkley parameter to the experimental data for shear rates < 140 s-1, gives parameter values

$$\begin{aligned} \tau_0 &= 0.6327 \\ K &= 0.1086 \\ n &= 0.4531 \end{aligned} \tag{3.3}$$

Comparison of the Herschel-Bulkley model with these parameters and the experimental data with drilling fluid containing 2.5% Bentonite at 80°C is shown in Figure 3.4.

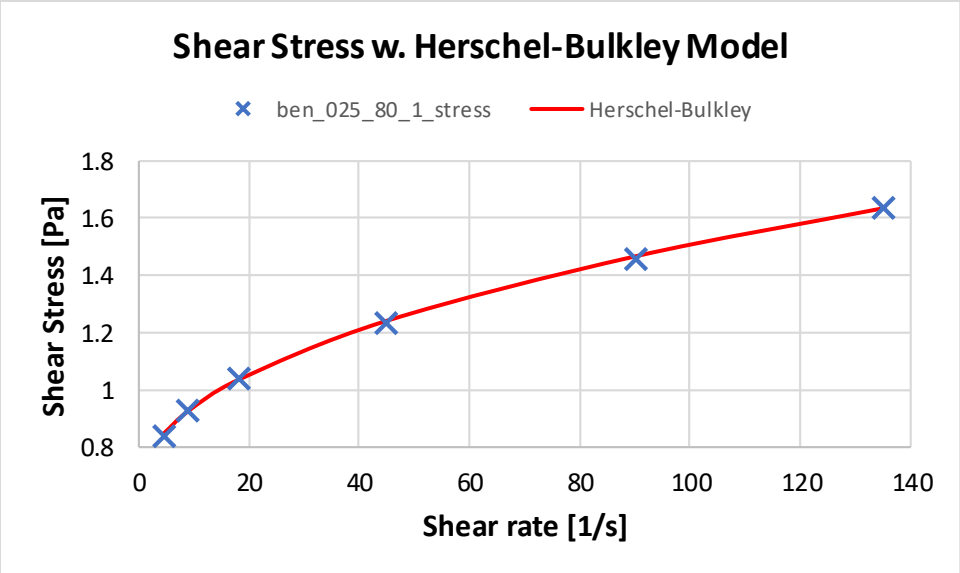

Figure 3.4: The drilling fluid tested in GeoDrill D1.3 is modelled with the Herschel-Bulkley model

1D implementation:

For the 1D implementation, the effects of the non-Newtonian fluid are taken into account through modified expressions for the calculation of friction factors.

Single-phase Newtonian fluids:

Calculation of the friction factor can have a large impact on the results and is a topic which has attracted a significant amount of research for many decades, as evidenced by for example review papers such as [6]. In most cases, the friction factor is calculated by different equations depending on whether the flow regime is laminar or turbulent. As the flow in a straight pipe with circular cross-section turns turbulent around Re=2320, it is common to use the Hagen-Poissueille equation for Re<2320. For turbulent flows, i.e. Re>2320, the most common method to calculate the friction factor is the Colebrook-White equation. However, the Colebrook-White equation is implicit and requires numerical iterations to be carried out for each element, for each iteration in each timestep, which can be time consuming. To overcome this, a non-iterative approximation provided by Haaland has been used for the turbulent regime. While these approximations are reasonably accurate for Re<2000 and

Re>4000, the transitional regime 2000<Re<4000 is poorly approximated. To overcome this, a three-regime approach [7] has been implemented, wherein the transitional regime is a weighted combination of the laminar and turbulent friction factors. To summarise, the flow friction factor in circular pipes is calculated as follows for single-phase Newtonian fluids:

$$f = f_L = \frac{64}{Re} \qquad Re < 2000\ (laminar\ flow) \tag{3.4}$$

$$f = f_t = \left\{-1.8log_{10}\left[\frac{6.9}{Re} + \left(\frac{\varepsilon}{3.7D}\right)^{1.11}\right]\right\}^{-2}, Re > 4000\ (fully\ turbulent\ flow) \tag{3.5}$$

$$f = yf_t + (1-y)f_L\ ,\ \ y = \frac{Re}{2000} - 1\ \ ,\ \ 2000 < Re < 4000\ (transitional\ flow) \tag{3.6}$$

where ε is the pipe wall roughness, D is the pipe diameter, and ε /D is the relative roughness. Notice that the Darcy-Weisbach definition of the friction factor is used, wherein the pressure drop is calculated as

$$\Delta p = f\rho\frac{Lv^2}{2D} \tag{3.7}$$

where L is the pipe length and v is the flow speed. For laminar flows, this gives

$$\Delta p = f\rho\frac{Lv^2}{2D} = 32\mu\frac{Lv}{D^2} \tag{3.8}$$

For water at 80°C in a typical 3.5 inch drill pipe [8], the pressure drop has been calculated with both the Flowphys1D code and with expression (3.8), see Figure 3.5 below. The input parameters for this case are:

$$\begin{gathered} L = 1000\ [m] \\ Inner\ diameter\ D = 66.04\ [mm] \\ \mu = 3.385e-4\ [Pa*s] \end{gathered} \tag{3.3}$$

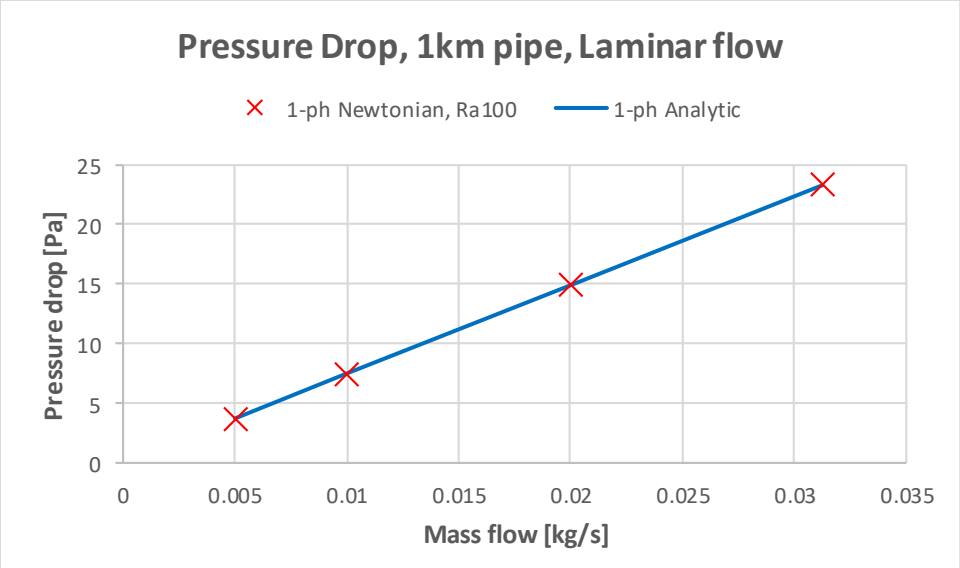

Figure 3.5: Comparison of Flowphys1D calculations with analytic expression for laminar flow

Single-phase non-Newtonian fluids:

For single-phase non-Newtonian fluids in pipes with circular cross-sections, the friction factor using the Herschel-Bulkley model is calculated as follows [9, 10]:

$$Re_{HB} = \frac{\rho v D_{eff-HB}}{\mu_a} \tag{3.103}$$

$$D_{eff-HB} = \frac{4n_a}{3n_a + 1} D \tag{3.11}$$

$$\mu_a = K \left(\frac{8v}{D_{eff-HB}} \right)^{n_a - 1} \tag{3.12}$$

$$n_a = \frac{nK \left(\frac{8v}{D} \right)^n}{\tau_0 + K \left(\frac{8v}{D} \right)^n} \tag{3.13}$$

where the values of the fluid model parameters n, K, and τ_0 are taken from the experimentally derived data in Eq. 3.3. The modified Reynolds' number Re_{HB} and D_{eff-HB} then replace Re and D in equations (3.4)-(3.6).

The pressure drop has been calculated for the same pipe as above and is shown in Figure 3.6 for low flow rates and in Figure 3.7 for high flow rates. As expected, the difference in pressure drop is much larger at low flow rates. Two different surface roughnesses have been used: a rather rough surface with absolute roughness 100μm, and a fine polished surface with absolute roughness 1 μm.

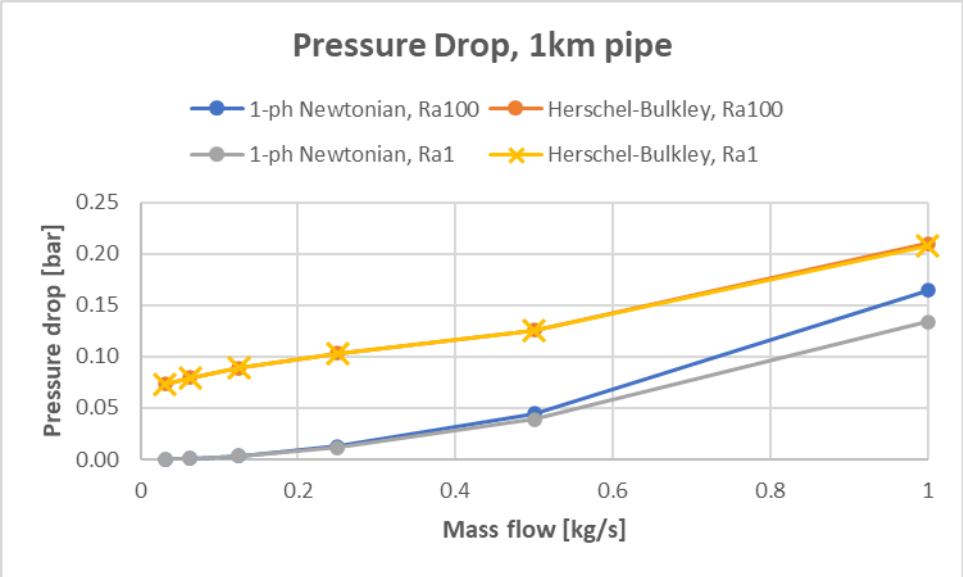

Figure 3.6: Pressure drop comparisons for 1-phase Newtonian and non-Newtonian with HB-model for low flow rates for a 1km pipe with drilling fluid containing 2.5% Bentonite at 80°C

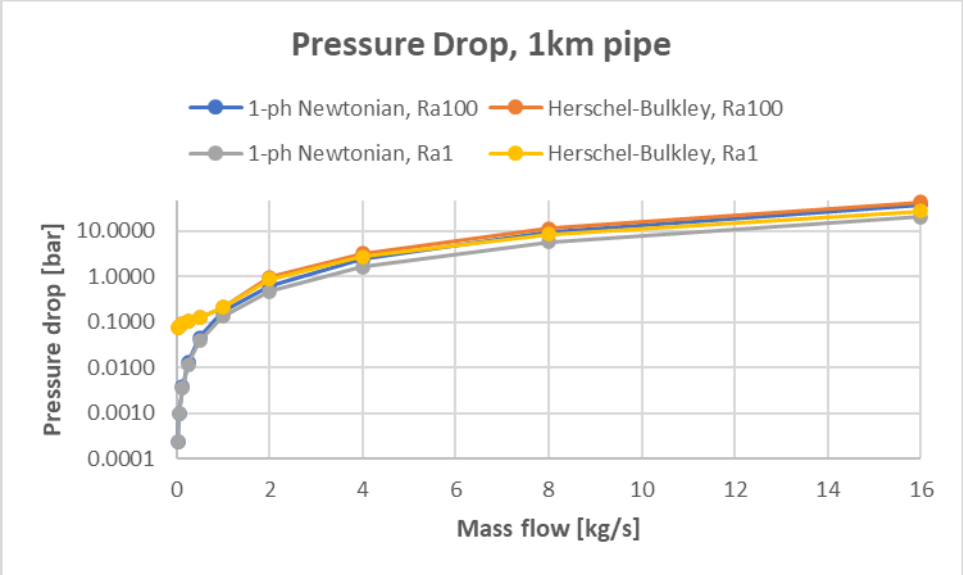

Figure 3.7: Pressure drop comparisons for 1-phase Newtonian and non-Newtonian with HB-model for high flow rates for a 1km pipe with drilling fluid containing 2.5% Bentonite at 80°C

Two-phase non-Newtonian fluids

For two-phase flows where the liquid is non-Newtonian, the friction factor is again calculated by using a modified Reynold's number $\overline{Re}_{HB}$ in equations (3.4)-(3.6):

$$\overline{Re}_{HB} = \frac{\bar{\rho}\bar{v}D_{eff-HB}}{\bar{\mu}_a} \tag{44}$$

where the mixture density $\bar{\rho}$ is calculated as

$$\bar{\rho} = \alpha_g\rho_g + \alpha_l\rho_l \tag{55}$$

where α_g and α_l are the volume fractions of gas and liquid. The viscosity is calculated as

$$\bar{\mu}_a = x\mu_g + (1-x)\mu_a\,, \tag{66}$$

where x is the mixture mass fraction,

$$x = \frac{\dot{m}_g}{\dot{m}_g + \dot{m}_l} \tag{77}$$

The mixture flow velocity is calculated as

$$\bar{v} = \frac{\dot{\bar{m}}}{\bar{\rho}A} \tag{88}$$

where $\dot{\bar{m}}$ is the mass flow rate of the gas-liquid mixture. For the homogeneous two-phase flow model, the velocity and pressure are the same for both phases:

$$\bar{v} = v_g = v_l \tag{3.19}$$

For the drift-flux model, there is a slip velocity between the phases. In the current Flowphys1D implementation, the model by Fabre and Line [11] is used:

$$v_g = C_o\bar{v} + v_d \tag{3.20}$$

$$C_o = \frac{2.27}{1+\left(\frac{\overline{Re}}{1000}\right)^2} + \frac{1.2}{1+\left(\frac{1000}{\overline{Re}}\right)^2}\ , \qquad \text{and} \quad v_d = 0 \tag{3.21}$$

The pressure drop has been calculated for the case of two-phase flows, with 1% mass fraction of gas in a pipe with pressure 10 bar. The liquid part of the fluid is assumed to be the bentonite-based drilling fluid, with 2.5% bentonite. Temperature is 80°C, i.e. the liquid part of the fluid is modelled with the Herschel-Bulkley model using the same parameters as above. Results for flows in the 1km long pipe are shown in Figure 3.8 for low flow rates and in Figure 3.9 for high flow rates. The surface roughness has been set to 100μm, i.e. a rather rough surface as can perhaps be expected inside a drill string driven by recycled drilling mud. As expected, the two-phase flow shows much larger pressure drop than single-phase flows.

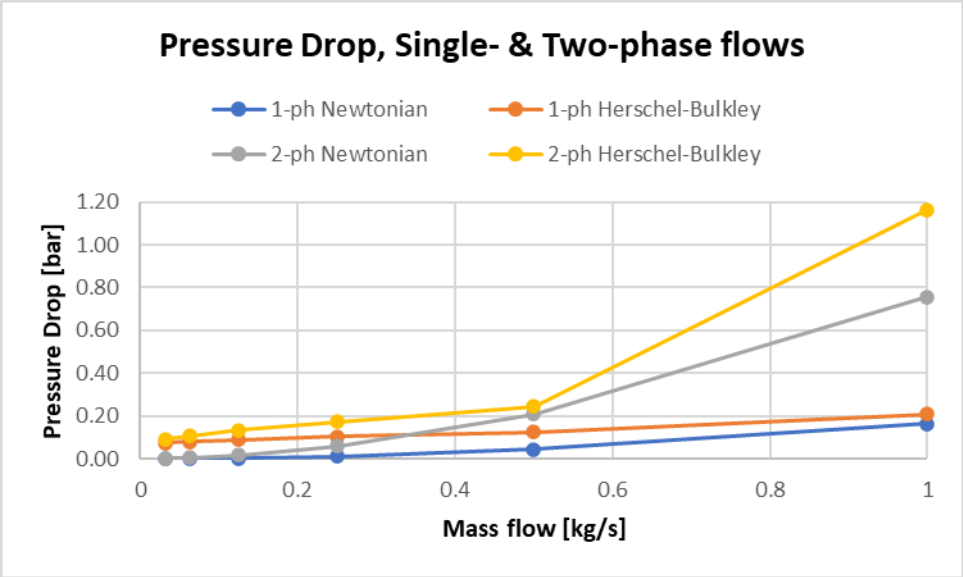

Figure 3.8: Pressure drop comparisons for 1-phase and 2-phase flows, where the liquid part of the fluid is either Newtonian (water) or non-Newtonian (water + bentonite) modelled with the Herschel-Bulkley model.

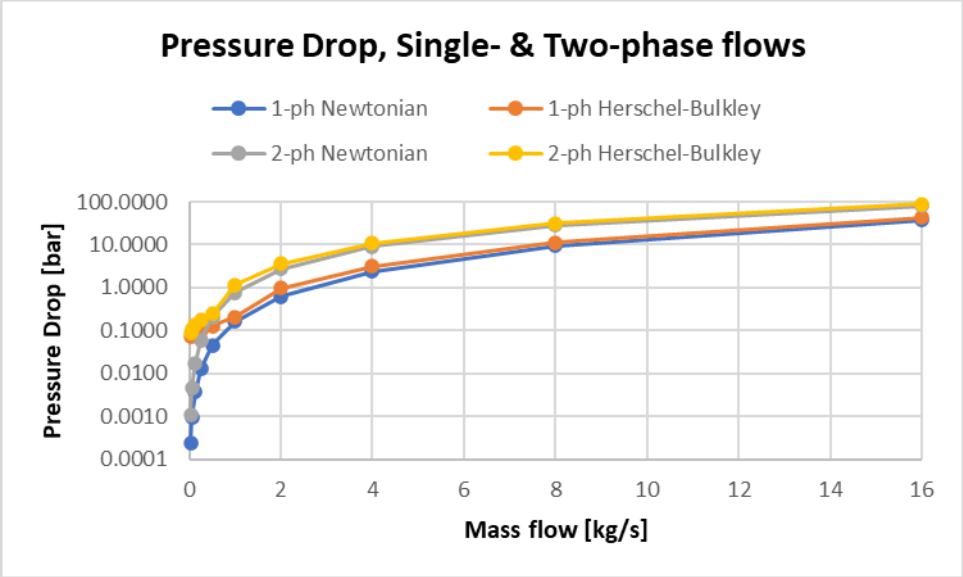

Figure 3.9: Pressure drop comparisons for 1-phase and 2-phase flows, where the liquid part of the fluid is either Newtonian (water) or non-Newtonian (water + bentonite) modelled with the Herschel-Bulkley model.

3.3 Annulus flow pressure loss model

The space between the drill string and the wellbore forms an annulus. With the inner diameter denoted D_i and the outer D_o , the hydraulic diameter for an annulus is

$$D_h = D_o - D_i \tag{3.22}$$

To calculate the pressure losses in the annulus, we use the same approach as for pipes with circular cross-sections, but with modifications to the expression for the friction factor. The Reynolds' number to be used in the friction factor calculation is

$$Re = \frac{\rho v D_h}{\mu} \tag{3.23}$$

For both single- and two-phase flows, the pressure loss in an annulus is modelled by modifying the friction factor with a geometric correction term [12], i.e.

$$f = k_g f \tag{3.24}$$

The annulus geometric correction term for laminar flows is

$$k_g = \frac{(1 - D_r)^2}{1 + D_r^2 + \frac{1 - D_r^2}{ln(D_r)}} \tag{3.25}$$

where D_r is the diameter ratio,

$$D_r = \frac{D_i}{D_o} \tag{3.26}$$

The annulus geometric correction term for turbulent flows is

$$k_g = (0.0786 D_r^3 - 0.209 D_r^2 + 0.184 D_r + 1) \tag{3.27}$$

Two-phase fluids

For two-phase fluids, the Reynolds' number is calculated as

$$\overline{Re} = \frac{\bar{\rho}\bar{v}D_h}{\bar{\mu}_a} \tag{3.28}$$

Combining with equations (3.4)-(3.6) gives the friction factor. Calculations for the pipe above, with a diameter ratio $D_r = 0.5$ are shown in Figure 3.10, and with diameter ratio $D_r = 0.9$ in Figure 3.11. As can be expected, the pressure drop is significantly larger in an annulus than in the circular pipe. Results for a two-phase flow are also shown in Figure 3.12, and just like in the case with circular pipe, the pressure drop increases with the two-phase flow due to higher velocities, as the mass flow is kept to the same constant value for both the single- and two-phase flows.

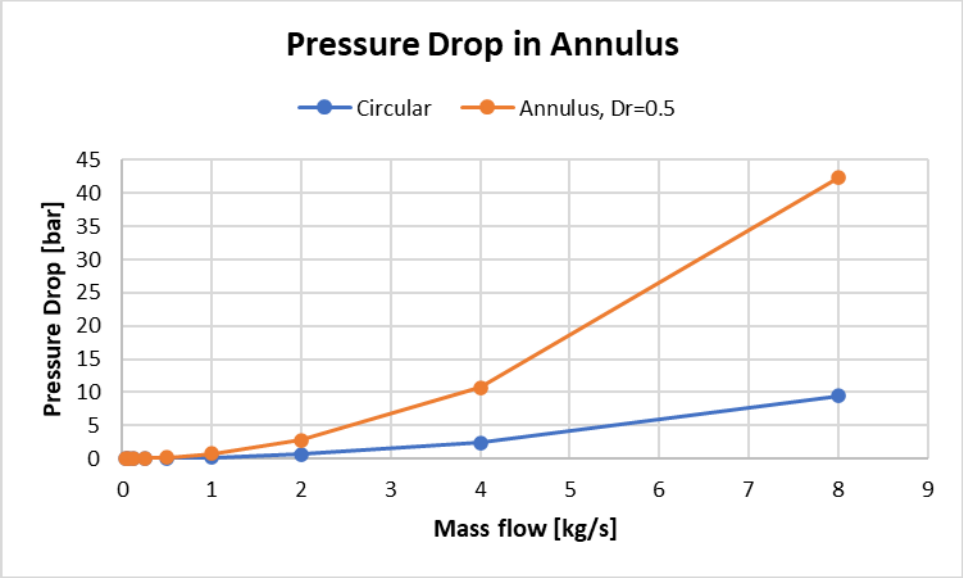

Figure 3.10: Pressure drop for circular vs. annular pipe with diameter ratio Dr=0.5. Absolute surface roughness Ra=100μm

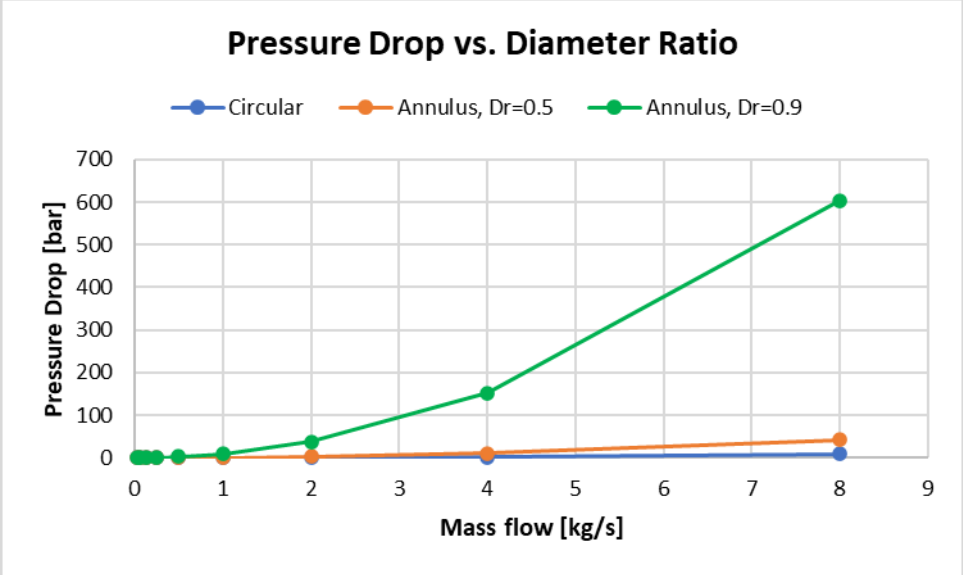

Figure 3.11: Pressure drop for annular pipe with large diameter ratio, Dr=0.9. Absolute surface roughness Ra=100μm

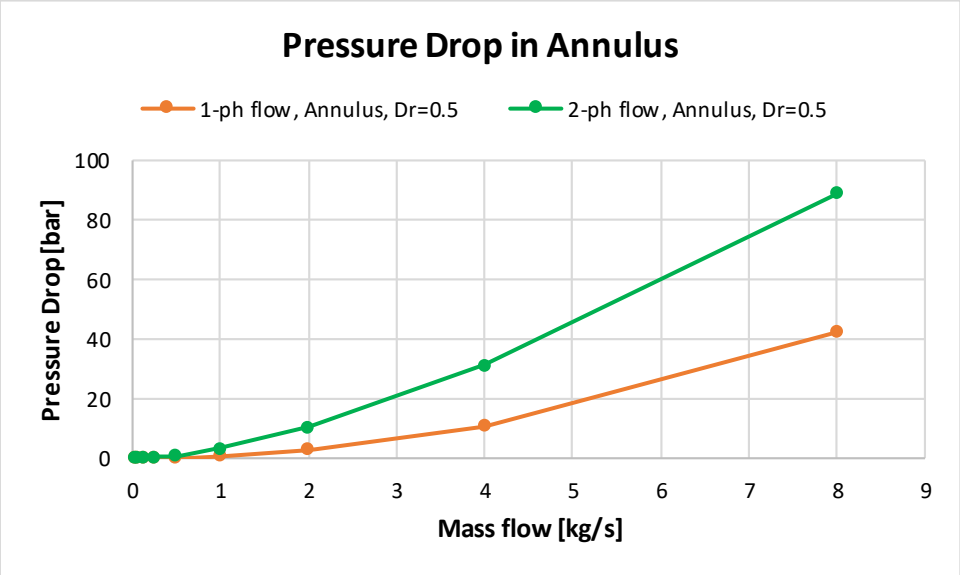

Figure 3.12: Pressure drops for single- and two-phase flows in an annular pipe with Dr=0.5. Absolute surface roughness Ra=100µm

3.4 Annulus flow heat transfer model

The temperature along the pipes and along an annulus is calculated by solving the energy equation, see Eq. 2.3.

There is a heat flux from the rock formation to the fluid in the annulus and inside the drill string, see Figure 3.13, where r_1 and r_2 are the inner and outer radii of the drill pipe, r_3 and r_4 are the inner and outer radii of the annulus, and r_5 represents a certain distance into the rock formation.

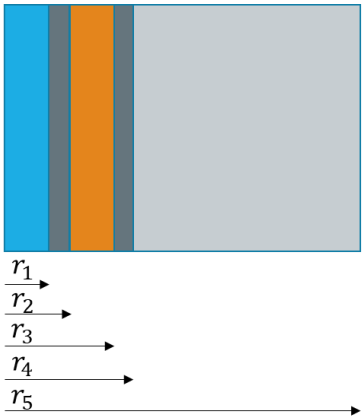

Figure 3.13: Layers in drill pipe and annulus

The heat fluxes from the drill pipe fluid to the annulus fluid and from the annulus fluid to the rock formation are calculated from

$$q_{FD-FA} = \frac{T_{Fluid\_drill} - T_{Fluid\_annulus}}{\frac{1}{2\pi r_1 L h_1} + \frac{ln\frac{r_2}{r_1}}{2k_A \pi L} + \frac{1}{2\pi r_2 L h_2}} \tag{3.29}$$

$$q_{FA-Rock} = \frac{T_{Fluid\_annulus} - T_{Rock}}{\frac{1}{2\pi r_3 L h_3} + \frac{ln\frac{r_4}{r_3}}{2k_B\pi L} + \frac{ln\frac{r_5}{r_4}}{2k_C\pi L}} \quad (3.30)$$

where q is heat loss per meter pipe [W/m], k_A is the conductivity of the drill pipe wall, k_B the conductivity of the liner (if any) between the annulus and the rock formation, k_C is the conductivity of the rock formation, h_1 is the heat transfer coefficient between the fluid and the inner drill pipe wall, h_2 is the heat transfer coefficient between the outside of the drill pipe and the annulus, and h_3 is the heat transfer coefficient between the annulus and the liner (or the rock formation in case of no liner).

The heat transfer coefficients are calculated from

$$h = \frac{Nu * k_F}{D_h} \quad (3.31)$$

$$h_2 = h_3 = \frac{Nu * k_F}{D_h} \quad (3.32)$$

where Nu is the Nusselt number, k_F is the thermal conductivity of the fluid, and D_h is the hydraulic diameter, which is

$$D_h = D = 2r_1 \quad (3.33)$$

for the heat transfer coefficient inside the drill pipe and

$$D_h = D_o - D_i \quad (3.34)$$

for the heat transfer coefficients in the annulus.

For laminar flow, the Nusselt number can be calculated from

$$Nu = 3.66 + \frac{0.065RePr\frac{D_h}{L}}{1 + 0.04\left(RePr\frac{D_h}{L}\right)^{2/3}} \quad (3.35)$$

For long pipes with uniform surface temperature, the Nusselt number can be approximated by

$$Nu = 3.66 \quad (3.36)$$

For turbulent flows, the Gnielinski [12] correlation gives

$$Nu = \frac{\left(\frac{f}{8}\right)(Re - 1000)\,Pr}{1 + 12.7(Pr^{\frac{2}{3}} - 1)\sqrt{f/8}} \quad (3.37)$$

where f is the friction factor. The Gnielinski correlation is valid also in the transitional region, for $2300 < Re < 5\text{x}10^6$ and in the Prandtl number range, $0.5 < Pr < 2000$.

The molecular Prandtl number Pr is calculated from

$$Pr = \frac{\mu C_P}{k_F} \quad (3.38)$$

For two-phase flows, the mixture Reynolds number, mixture viscosity, mixture heat capacity, mixture conductivity, and mixture Prandtl number are used to calculate the heat transfer coefficients, i.e.

$$\bar{C} = xC_g + (1-x)C_l \tag{3.39}$$

$$\bar{k} = xk_g + (1-x)k_l \tag{3.40}$$

3.5 Hammer tool assembly

The hammer tool assembly consists of several different parts as shown in Figure 3.14.

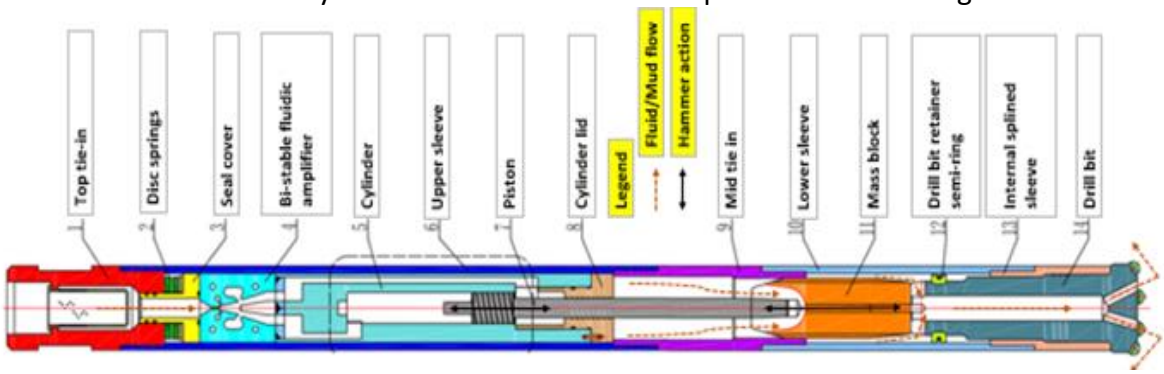

Figure 3.14: Hammer tool assembly

There is a significant pressure drop over the hammer tool assembly. Because the flow field and the piston internal to the hammer tool oscillate, the pressure drop over the whole assembly will also oscillate. To simulate the flow through the whole drill string during drilling operations, it is necessary to implement models for the whole hammer tool assembly. The hammer tool design is developed in GeoDrill WP4. While the full design is not finalised yet, experiments have been carried out for a simplified percussion mechanism as shown in Figure 3.15. Using the FlowPhys3D software, CFD fluid-structure interaction calculations have also been carried out as shown in Figure 3.16.

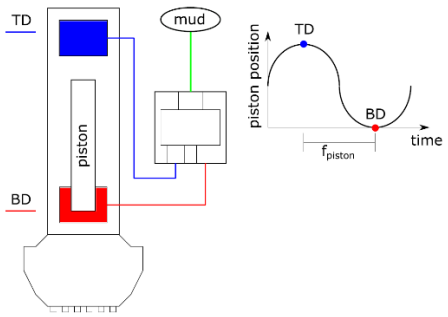

Figure 3.15: Schematic view of the GeoDrill percussion system experimental setup at Fraunhofer IEG in Bochum, Germany [13]

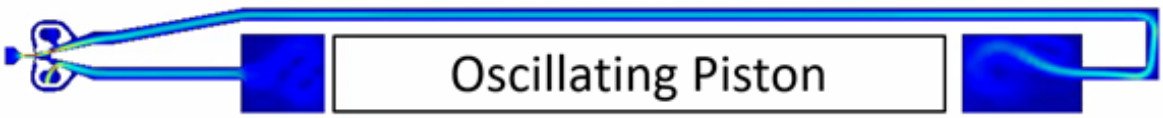

Figure 3.16: Velocity contours: CFD Fluid-Structure interaction analysis of percussion mechanism [13]

Through curve fitting to data, the following models have been derived:

$$-\Delta p_{mean} = 0.0016Q^2 + 0.0023Q - 0.0201 \quad (3.41)$$

$$freq = 0.0421Q + 0.1214 \text{ Hz} \quad (3.42)$$

$$\Delta p_{Amplitude} = 0.15\Delta p_{mean} \quad (3.43)$$

where Q is the volumetric flow rate. These models will be extended and improved when more data points become available.

4. CONCLUDING REMARKS

A new engineering analysis software for geothermal flow assurance is under development by Flowphys AS. This software is capable of simulating single-phase and multi-phase dynamic (time-dependent) flows in pipe networks. The software is based on solving the conservation equations for mass, momentum, and energy. Conservation and other criteria are also applied at the pipe network junction nodes.

The fundamentals of the flow assurance software, Flowphys1D, have been briefly described. The report also describes new models that have been developed for non-Newtonian fluids, flow and heat transfer in the annulus, and for the hammer tool assembly. In addition, the report also describes a Drill Module GUI which has been developed to simplify and speed-up end-user input for construction of the well and drill string geometries and meshes.

To showcase the newly developed models, simulations of test examples have been presented. These models will be further extended and tuned when experimental and field results data become available later in the project.

5. REFERENCES

1. H2020 GeoCoat, Grant Agreement LCE-GA-2018-764086, https://www.geo-coat.eu/
2. PHREEQC Ver. 3; "A computer Program for Speciation, Batch-Reaction, One-Dimensional Transport, and Inverse Geochemical Calculations", https://wwwbrr.cr.usgs.gov/projects/GWC_coupled/phreeqc/
3. P. Kjellgren, C.B. Jenssen, T. Peng, GeoDrill deliverable report D4.1 "Design and simulation of fluidic amplifier", Nov. 2019
4. Schlumberger Oilfield Glossary, https://glossary.oilfield.slb.com/Terms/h/herschel-bulkley_fluid.aspx
5. Kristján Friðrik Alexandersson and Jan Přikryl: GeoDrill D1.3 Rheology testing report, 31/8/2019
6. M. Asker, O.E. Turgut, M.T. Coban, "A review of non-iterative friction factor correlations for the calculation of pressure drop in pipes", Bitlis Eren Univ. J. Sci & Technology, 2014
7. M. Zaupa, "Thermo-hydraulic models and analyses for design optimization of cooling circuits and components of SPIDER and MITICA experiments", PhD thesis, 2016
8. Drill Pipe Specifications: http://www.drill-pipes.com/drill-pipe-specifications.php
9. J.C.M. Vidaur, "Experimental Study of Automated Characterization of Non-Newtonian Fluids", MSc thesis, 2018

10. Q.H. Nguyen and N.D. Nguyen, Incrompressible Non-Newtonian Fluid Flows, Continuum Mechanics – Progress in Fundamentals and Engineering Applications, InTech, 2012
11. Fabre, J., Line, A. Modeling of two-phase slug flow, Annu. Rev. Fluid Mech, 1992
12. O. Bratland, "Pipe Flow 1: Single-Phase Flow Assurance", 2009
13. F. Zhang, H. Begg, N. Kale, S. Irukuvarghula, V. Wittig, K. Mallin, B.A. Rodriguez, F. Chowdhury, M. A. Hoque, S.N. Karlsdottir, G.O. Boakye, P. Kjellgren, "Geo-Drill: Development of novel and cost-effective drilling technology for geothermal systems", WGC 2021